Electrostatic and Charge-Induced Methane Activation by a Concerted Double C−H Bond Insertion

Caiyun Geng,[†] Jilai Li,[*,†,‡] Thomas Weiske,[†] Maria Schlangen,[†] Sason Shaik,[*,§] and Helmut Schwarz[*,†]

[†]Institut für Chemie, Technische Universität Berlin, Straße des 17. Juni 135, 10623 Berlin, Germany
[‡]Institute of Theoretical Chemistry, Jilin University, Changchun 130023, PR China
[§]Institute of Chemistry and the Lise-Meitner-Minerva Center for Computational Quantum Chemistry, The Hebrew University of Jerusalem, 91904 Jerusalem, Israel

S Supporting Information

ABSTRACT: A mechanistically unique, simultaneous activation of two C−H bonds of methane has been identified during the course of its reaction with the cationic copper carbide, $[Cu−C]^+$. Detailed high-level quantum chemical calculations support the experimental findings obtained in the highly diluted gas phase using FT-ICR mass spectrometry. The behavior of $[Cu−C]^+/CH_4$ contrasts that of $[Au−C]^+/CH_4$, for which a stepwise bond-activation scenario prevails. An explanation for the distinct mechanistic differences of the two coinage metal complexes is given. It is demonstrated that the coupling of $[Cu−C]^+$ with methane to form ethylene and Cu^+ is modeled very well by the reaction of a carbon atom with methane mediated by an oriented external electric field of a positive point charge.
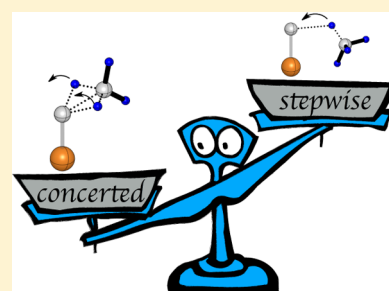
1. INTRODUCTION

We report herein an unprecedented, mechanistically unique Cu^+-mediated insertion of a carbon atom into two C−H bonds of methane to form ethylene in a single, barrier-less step. While the search for catalysts capable of directly transforming methane into more value-added commodities has been pursued for over a century, breaking the thermodynamically strong and kinetically inert C−H bond of methane under mild conditions and in a controlled fashion still constitutes a central challenge.[1,2] Considerable attention has been paid to the elucidation of mechanistic aspects pertinent to direct methane conversion, and tremendous progress has been made in the past decades.[3−10] In this context, classical hydrogen-atom transfer (HAT),[11,12] proton-coupled electron transfer (PCET),[13,14] as well as hydride transfer (HT)[15] scenarios have been proposed, and many of the key factors that control the reactivity have also been clarified. The knowledge under which conditions HAT, PCET, and HT are operative in the activation of methane not only deepens our mechanistic understanding but may also guide the rational design of appropriate catalysts, as the one discussed in this work.

Thus, it is well-known that free atomic carbon participates in abstraction, addition, and insertion reactions.[16] Experimentally,[17,18] ground-state $C(^3P)$ does not react with methane, in accord with theoretical findings that the reaction faces a barrier of 51 kJ mol^{-1}.[19] However, in its lowest electronically excited state, $C(^1D)$ (122 kJ mol^{-1} above ^3P) inserts into a C−H bond forming an $HCCH_3$ intermediate that rearranges to the global minimum ethylene at a collision energy of 25.3 kJ mol^{-1}.[17]

Metal complexes, capable of activating methane under thermal conditions in the gas phase,[20,21] have served as prototypical systems to probe the active sites in heterogeneous catalysis, the so-called "aristocratic atoms".[22,23] Recently, we succeeded in ligating atomic carbon by the strongly electrophilic atomic gold cation Au^+ to form in the gas phase the diatomic gold carbide $[Au−C]^+$.[15] Bare $[Au−C]^+$ reacts under thermal, single-collision conditions with methane with a reaction efficiency of 22% relative to the collision rate.[15] The reaction of singlet ground-state $[Au−C]^+$ with methane is confined to the singlet surface. Excited electronic states are much too high in energy to play a role. The electrophilic carbon atom in $[Au−C]^+$ serves as the reactive site, and the reaction features a conventional electrophilic insertion of carbon into one C−H bond of methane in the first C−H bond activation step, followed by a 1,2-hydrogen migration, forming an ethylene-metal complex $[Au(C_2H_4)]^+$, from which ethylene is finally evaporated. The sequential cleavage of two C−H bonds of an alkane is typical for alkane-to-alkene conversions. To the best of our knowledge, there exists only one example for the concerted activation of two C−H bonds; some benzynes are capable of bringing about the concerted removal of two vicinal hydrogen atoms from a cycloalkane.[24]

This reactivity patterns of gold raises immediate questions about its lighter congener, copper. For example, does the corresponding carbide $[Cu−C]^+$ react the same way with methane as $[Au−C]^+$ or are there any noticeable differences? Furthermore, what role is played by the metal ion in the C-insertion when
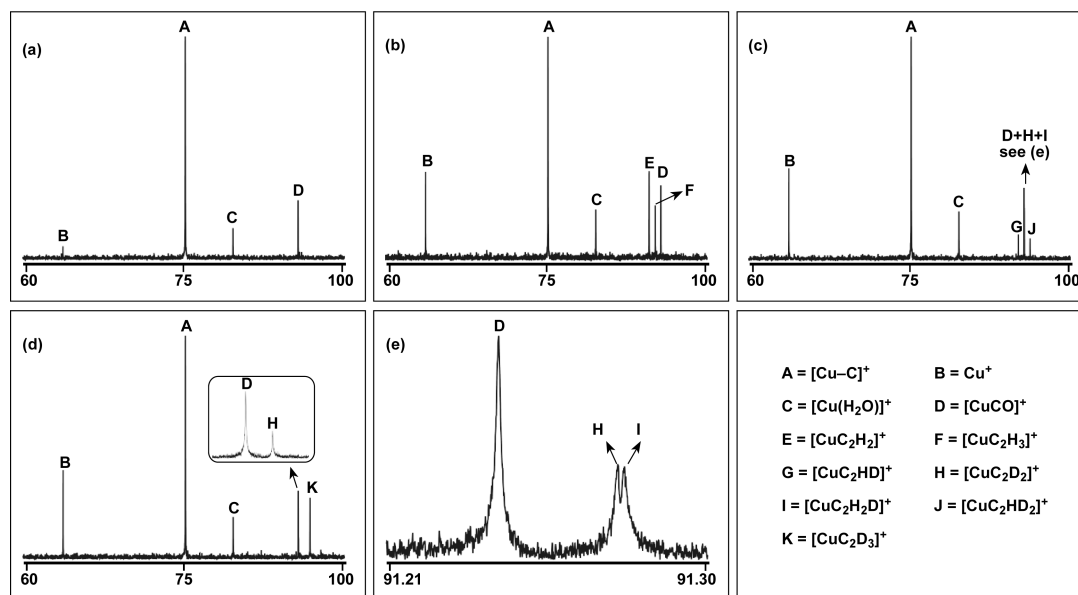
Figure 1. Mass spectra for the thermal reactions of $[Cu-C]^+$ with (a) argon, (b) CH_4, (c) CH_2D_2, and (d) CD_4 at a pressure of 3.0×10^{-9} mbar and a reaction time of 3 s, respectively. (e) High-resolution mass spectrum of $m/z = 91$. The x axes refer to m/z.
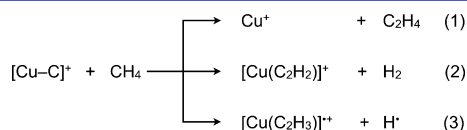
compared with that in the reaction of bare $C(^1D)$ with methane?

Herein we report our surprising findings on the reaction of bare $[Cu-C]^+$ with methane as revealed in a combined experimental/computational approach. All the gas-phase experiments were performed by using Fourier transform ion cyclotron resonance mass spectrometry (FT-ICR MS) under thermal, single-collision conditions. Mechanistic aspects were elucidated by high-level quantum mechanical calculations; the root cause of the distinct mechanistic variants of the two systems $[M-C]^+/CH_4$ (M = Cu and Au) has been clarified. We explored the feasibility and mechanistic aspects of the two C−H bond insertions for the $C(^1D)/CH_4$ and $[M-C]^+/CH_4$ (M = Cu and Au), in order to obtain a deeper understanding of this unusual two-bond activation reaction. We also considered the silver-cation case; however, we did not succeed in producing the bare $[Ag-C]^+$ in our instrumental setup in amounts sufficient to perform reactions with CH_4. Finally, we showed that the role of Cu^+ can be modeled faithfully by a positive point charge that acts as an external electric field[25−29] mediator in the double C−H bond insertion.

2. RESULTS AND DISCUSSION

The FT-ICR mass spectra in Figure 1 show the reactions of mass-selected, thermalized $[CuC]^+$ ions ($m/z = 75$) with isotopologues of methane. To differentiate between reactions of the parent ion with background gases, reference spectra were recorded with the inert gas argon.

As indicated in the reference spectrum in Figure 1a, both carbon-atom transfer (CAT) and oxygen-atom transfer (OAT) processes take place in the reaction of $[Cu-C]^+$ with background gases. When treating $[Cu-C]^+$ with CH_4, CH_2D_2 or CD_4, as in Figure 1b−e, the signal corresponding to CAT is significantly enhanced (eq 1); in addition, a new signal ($m/z = 89$) appears representing the formal uptake of a carbene unit from methane accompanied by the liberation of H_2 (eq 2). Furthermore, a signal ($m/z = 90$) is present which has been assigned to $[Cu(C_2H_3)]^{\bullet+}$ generated under the concomitant elimination of atomic $H^\bullet$ (eq 3). In addition to exact mass

$$[Cu-C]^+ + CH_4 \longrightarrow \begin{cases} Cu^+ + C_2H_4 & (1) \\ [Cu(C_2H_2)]^+ + H_2 & (2) \\ [Cu(C_2H_3)]^{\bullet+} + H^\bullet & (3) \end{cases}$$

measurements, the identity of the ionic product species in the observed reactions has been confirmed by labeling experiments shown in Figure 1c−e.

The rate coefficient for the reaction, $k([Cu-C]^+/CH_4)$, is estimated to 5.2×10^{-10} cm^3 molecule^{-1} s^{-1}; after considering the contribution of background gases, this corresponds to a reaction efficiency of 44% relative to the collision rate.[30−32] Owing to the uncertainty in the determination of the absolute pressure, an error of $\pm 30\%$ is associated with these measurements. For the couple $[Cu-C]^+/CD_4$, the rate constant decreases to $k = 4.4 \times 10^{-10}$ cm^3 molecule^{-1} s^{-1}; thus, the intermolecular kinetic isotope effect (KIE) derived from the $[Cu-C]^+/CH_4/CD_4$ systems amounts to KIE = $k_H/k_D = 1.2$. As to the branching ratio (eqs 1−3), these are affected by both the reaction time and the varying contribution of background. However, as shown in Figure 1a,b the major process corresponds to the generation of Cu^+.

In order to obtain mechanistic insight into the $[Cu-C]^+$ mediated C−H bond activation of methane, high-level quantum mechanical (QM) calculations were carried out. Four pathways were considered in this study. Three of them (pathways **A**, **B**, and **C**), being stepwise in nature, are initiated by standard single C−H bond activation via classical HAT or HT scenarios; they are relegated to the Supporting Information for the sake of conciseness (Figure S1 and Table S1). As the fourth (pathway **D** in Figure S1) is unprecedented and mechanistically unique, we therefore focus on it herein.

In contrast to $[Au-C]^+$, the ground state of diatomic $[Cu-C]^+$ corresponds to the triplet state; its lowest excited singlet state is 14 kJ mol^{-1} higher in energy. While the reaction of $[Cu-C]^+/CH_4$ starts on the triplet surface, it is subject to a two-state reactivity (TSR)[33] mechanistic scenario. As shown in Figure 2, the reaction has its origin on either singlet or triplet separated reactants. These two surfaces cross at the
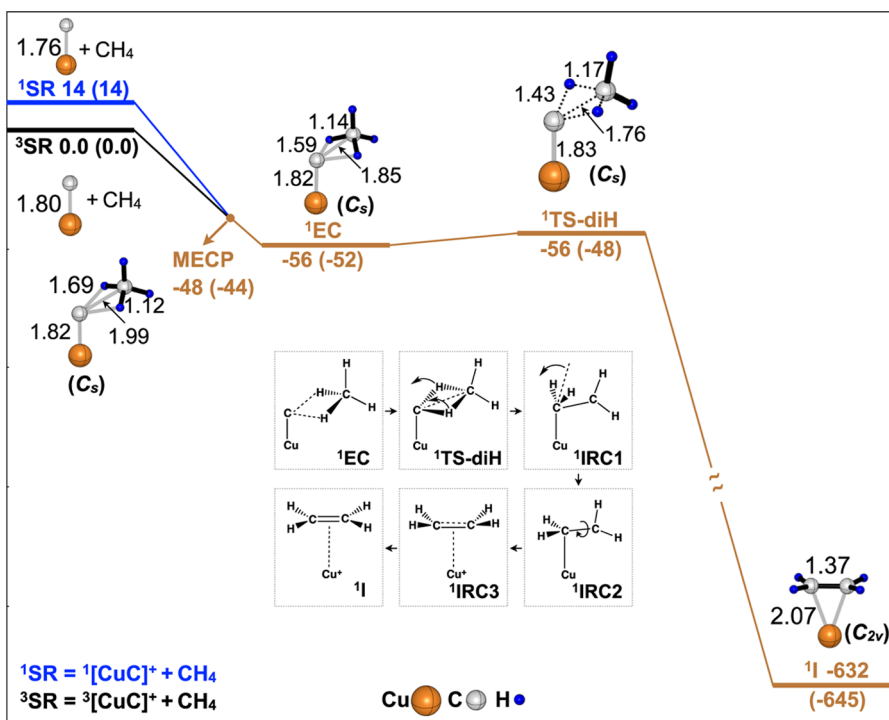
Figure 2. CCSD(T)//B2PLYP-calculated potential energy profile for the synchronous two C–H bond insertion step of $[Cu-C]^+$/CH_4. Key ground-state structures with selected geometric parameters are also provided. Relative enthalpies ($\Delta H_{298\ K}$ in kJ mol^{-1}), corrected for contributions of zero-point vibrational and thermal energies, of the reaction intermediates and transition states are given relative to the separated reactants $^3[Cu-C]^+$ and CH_4. Relative electronic structure energies (ΔE in kJ mol^{-1}), without zero-point vibrational and thermal energies, are also provided in parentheses. Charges are omitted for the sake of clarity. The inset shows the schematic diagram of the bond breaking/making in the single step along IRC calculations.

minimum-energy crossing point,[34] **MECP** (-48 kJ mol^{-1}), that mediates a spin flip from the triplet to the singlet surface and generates ^{1}**EC**. The subsequent reaction proceeds in an unprecedented way: The electrophilic carbon atom of $^1[Cu-C]^+$ simultaneously inserts into the two C–H bonds of methane via ^{1}**TS-diH** (-56 kJ mol^{-1}). In the same step, the nascent CH_2 bends backward, while the CH_2 group remaining of methane rotates by 90° along the C–C axis, thus giving rise to the ethylene-copper complex ^{1}**I** (-632 kJ mol^{-1}). The latter corresponds to the global minimum on the potential energy surface.

Note that the transition state (^{1}**TS-diH**) for this concerted mechanism involves, in a single step, the simultaneous breaking of two C–H bonds of methane, the formation of two new C–H bonds and a C=C double bond, and the transformation of a $\sigma_{(Cu-C)}$ bond into a π interaction of copper with the newly formed C=C double bond (Figure S2). Nevertheless, ^{1}**TS-diH** still provides the lowest barrier among the four pathways considered (Figure S1).

Since gold, due to a strong relativistic effect,[35,36] is more electronegative than copper,[37,38] the carbon atom of $[Au-C]^+$ is more electrophilic than that of $[Cu-C]^+$. Thus, for electrophilic reactions, when carbon serves as a reactive site the reactivity of $[Au-C]^+$ is expected to be higher. However, when gold is replaced by copper, the reactivity of $[Cu-C]^+$/CH_4 does not decrease; rather, it increases by nearly a factor of 2.[15] This indicates that different mechanisms are operative for both systems. While the concerted mechanism for $[Au-C]^+$ had not been considered in the previous study,[15] a reconsideration of the $[Au-C]^+$/CH_4 couple reveals that the concerted transformation is not competitive with the stepwise process (Table 1); as shown earlier,[15] the reaction of $[Au-C]^+$

Table 1. Rate-Limiting Barriers (kJ mol^{-1}) in the Concerted and Stepwise Mechanisms of the Three Systems^a

reactants	concerted	stepwise
$^1[Au-C]^+ + CH_4$	2	-31
$^1[Cu-C]^+ + CH_4$	-48	-18
$C(^1D) + CH_4$	103	17

^{a}Relative electronic structure energies, with respect to the ground-state separated reactants, are obtained at the CCSD(T)//B2PLYP level of theory. Note that zero-point vibrational energies and thermal corrections are not considered.

with methane occurs in a stepwise fashion. Thus, as far as the mechanistic aspects are concerned, copper behaves differently than gold.

The preferences in favor of stepwise versus concerted mechanisms for the reactions of $[Au-C]^+$ versus $[Cu-C]^+$ with methane (Table 1) can be ascribed to the large difference between the bond dissociation energies (BDEs) of the two carbides $[M-C]^+$ (M = Cu and Au). The BDE of $[Au-C(^1D)]^+$ amounts to 501 kJ mol^{-1} and is 172 kJ mol^{-1} higher than that of $[Cu-C(^1D)]^+$ (Table S2).[39] The Au–C bond is more covalent than the corresponding Cu–C bond (Figure S3); this is also confirmed by the Wiberg bond-order index analysis (WBI = 0.84 for $[Au-C]^+$ vs 0.50 for $[Cu-C]^+$). Therefore, the gold cation is more reluctant to loosen its σ-bond to the carbon atom. As breaking the σ-bond of $[Au-C]^+$ becomes more difficult, it impedes the stabilizing electronic reorganization of the transition state of the concerted mechanism as described above. This was verified here by starting from the optimized structure of $[Au-C]^+$, while artificially elongating the distance between the gold and the carbon atom until such point

where the BDE reaches the value of $[Cu-C]^+$. For each such optimized artificial structure, the barrier $\Delta E^{\ddagger}$ of the concerted mechanism has been calculated. As Figure 3 shows, the
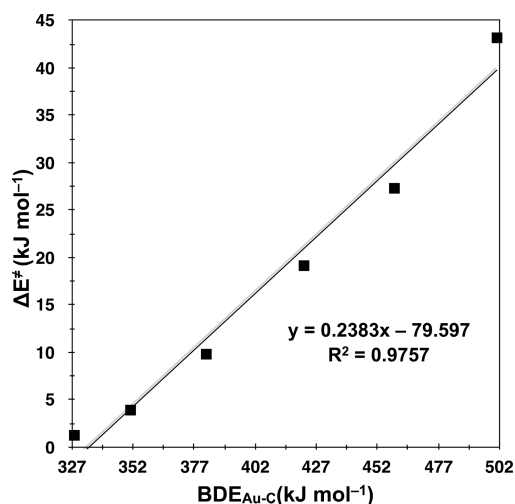

Figure 3. Plot of the barrier $(\Delta E^{\ddagger})$ of the concerted, two-bond insertion mechanism versus that of the simulated BDE of $[Au-C]^+$.

relationship between the so obtained BDE and $\Delta E^{\ddagger}$ is almost linear, and $\Delta E^{\ddagger}$ becomes smaller as the BDE of $[Au-C]^+$ decreases. Thus, the BDE of $[Au-C]^+$ has a significant impact on the barrier heights of the concerted pathway. The barrier is significantly lowered at a $BDE_{Au-C} < 350$ kJ mol^{-1}, thereby favoring the concerted pathway. Therefore, a small BDE of $[M-C]^+$ constitutes the root cause of the mechanistic switch from the stepwise to a concerted scenario for the insertion of an electrophilic carbon atom into two C−H bonds of methane. Note that an analysis of the quasi-restricted orbitals[40,41] also points to the electron pair of $\sigma(C-Cu)$ which is directly involved in the $\sigma(C-C)$ bond making (Figure S2); this supports the validity of our BDE argument.

In order to address the particular role of the metal cation during the course of the reaction of the carbon site of $[M-C]^+$ (M = Cu and Au) with methane, a comparison was made to the reaction of a free carbon atom with methane. High-level calculations show that the transition state for the synchronous insertion of a carbon atom in its lowest excited state $C(^1D)$ into two C−H bonds requires up to 103 kJ mol^{-1}; the initial single

C−H bond insertion is better described as a stepwise process which possesses a moderate barrier (Table 1 and Figure S4).

For the direct reaction $C(^1D) + CH_4$, the extremely unfavorable concerted mechanism can be attributed to the high energy level of the two degenerate electron acceptor orbitals of the singlet carbon atom. As shown in Figure 4a,b, the energy gap between the $\sigma(C-H)$ orbital of methane and the vacant C 2p orbital of $C(^1D)$ amounts to 1020 kJ mol^{-1}; in contrast, a value of 313 kJ mol^{-1} is obtained for the corresponding orbital in $[Cu-C]^+$. This severe energy mismatch between frontier symmetry-compatible orbitals in the $C(^1D)/CH_4$ couple prevents much stabilization of the corresponding transition state and is the root cause for the prohibitively high barrier. However, once Cu$^+$ is ligated to $C(^1D)$, the energies of the vacant 2p orbitals of carbon drop by more than 700 kJ mol^{-1}. This is of crucial importance for a better energy match between the frontier orbitals of the transition state for the concerted pathways. Thus, the stability of **^{1}TS-diH** for the concerted two C−H bond insertion process originates in the substantial orbital-mixing energy as well as in large electrostatic stabilization due to the significant charge transfer from CH$_4$ to C in $[Cu-C]^+$ in the TS ($0.62e^-$ is transferred; see Table S3). This combined orbital and electrostatic stabilization energy overrides the large deformation energy incurred due to the extensive structural reorganization of CH$_4$ (see Supporting Information on the analysis of the deformation and interaction energies in **^{1}TS-diH**).

As argued above (Figure 3), a smaller BDE($[M-C]^+$) corresponds to a higher reactivity toward methane via the concerted mechanism (Figure 3). When extrapolating the BDE of $[M-C]^+$ to 0, the difference between $[M-C]^+$ and $C(^1D)$ is merely the positive charge carried by the metal. Indeed, the charge on Cu in $[Cu-C]^+$ amounts to 0.80 (see Table S3), so the question is whether a positive point charge can take over the role of the atomic coinage metal cations.[42]

The answer to this kind of a "Gedankenexperiment" is provided herein. As shown in Figure 4c, a positive point charge placed in the vicinity of $C(^1D)$ has even a larger effect than Cu$^+$ in lowering the energy of the vacant C 2p orbital of $C(^1D)$. Moreover, in the presence of the field of the positive charge, the ground state of the carbon atom switches from triplet (^{3}P) to the singlet (^{1}D) state as the charge intensity increases (Figure S5).[43] Led by these results, we explored the energy difference between the encounter complex **^{1}EC** and the
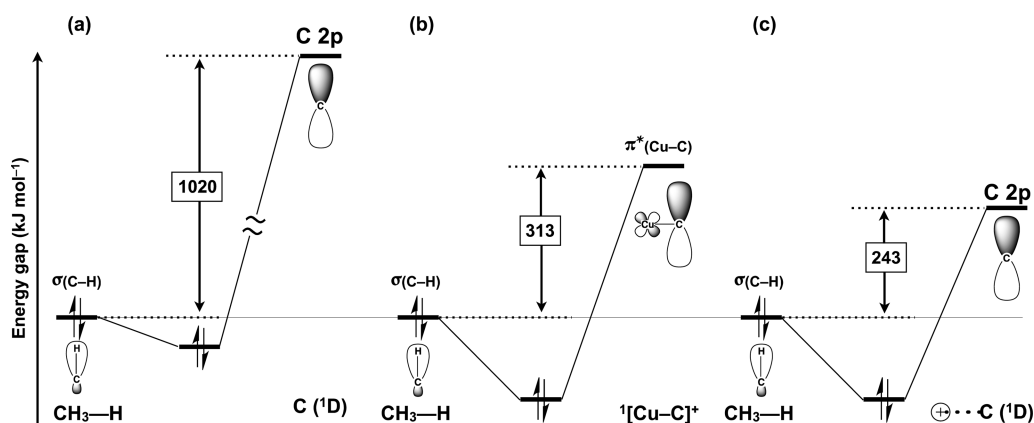

Figure 4. Energy gaps (kJ mol^{-1}) between the $\sigma(C-H)$ orbital of methane and (a) the vacant C 2p orbital of $C(^1D)$, (b) $[Cu-C]^+$, and (c) positive charge coupled $C(^1D)$.
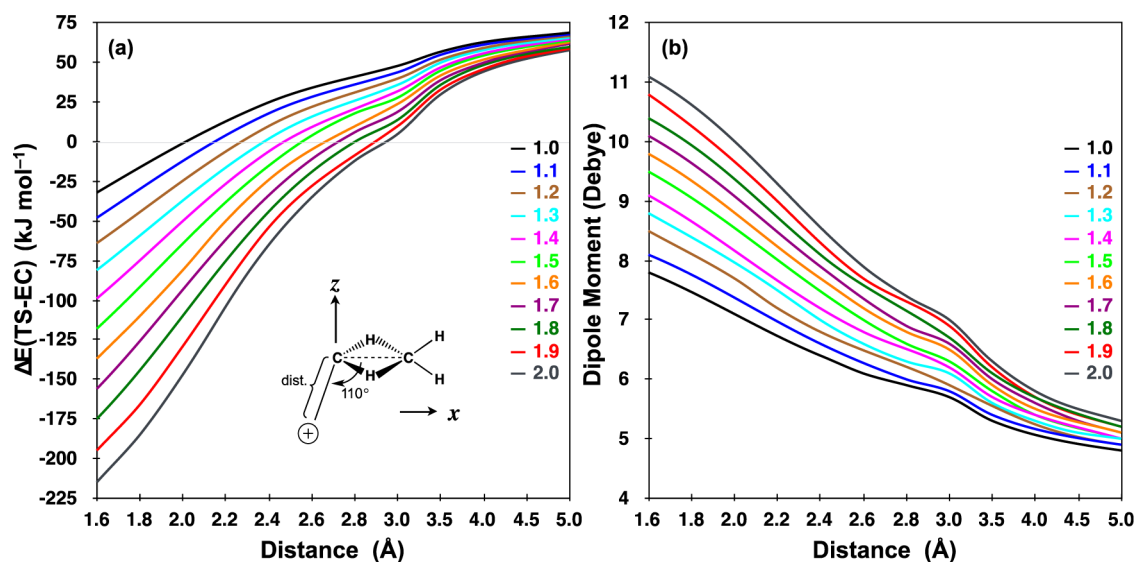
Figure 5. (a) Plot of the relative energies (kJ mol^{-1}) between the transition state and the encounter complex under the influence of a positive point charge. Charge intensities (1.0e−2.0e) are colored by black to gray; distances between the positive point charge and C(^{1}D) are in the range of 1.6−5.0 Å. Note that here the positive point charge is placed at the metal position of the [Cu−C]$^+$/CH$_4$ system, but the corresponding structures in the C(^{1}D) + CH$_4$ reaction are used. (b) The x-axis refers to the direction of the dipole moment of the transition state under the influence of a positive point charge. Color code and distance are the same as shown in panel a.

transition state ^{1}TS-diH under the influence of a positive point charge, varied between +1e to +2e. The result is visualized in Figure 5a. It clearly shows that the barrier diminishes as the point charge, which spawns an oriented external electric field (OEEF)[25−29] for the reacting particles, approaches the atomic C(^{1}D) in the direction drawn in the same figure. Increasing the magnitude of the point charge while keeping the distance constant has the same effect. As the OEEF strength is increasing, at a certain value the barrier vanishes, and the concerted mechanism becomes a barrier-free process (Table S4).

The positive point charge approaching the carbon center causes a significant charge transfer from methane toward the carbon atom compared to the nonpolar, unassisted reaction of C(^{1}D) with CH$_4$ (See Table S5). As the field strength of the point charge increases, the dipole moment of the transition state ^{1}TS-diH increases as well (Figure 5b). As a consequence, the weights of ionic structures of the transition state along the reaction axis are augmented, leading to electrostatic stabilization of the transition state.[42,44] The OEEF-induced dipole moment is obviously affected by its corresponding orientation. The largest attenuated barrier can thus be accomplished by tuning the alignment of the field's polarity (Figure S6).[26,42,45] Similar results were obtained by Coote et al. in the effect of remote charges on radical reactions.[46] Therefore, the enormous effect caused by this coinage metal can actually be modeled by a positive point charge serving as a reagent,[45] and the mechanistic switch could be accomplished by tuning the direction and intensity of the OEEF at will. Complementing our experimental findings of a metal-cation complexed carbon with the one calculated for a positive point charge, the effect of a negative point charge on the opposite site of the reacting carbon/methane couple was also considered. As expected, a substantial decrease of the reaction barrier is predicted (for details, see Figure S6e).

3. CONCLUSIONS

In summary, a synchronous insertion of an electrophilic carbon atom into two C−H bonds of methane has been discovered for

the first time in a combined experimental/computational study on the thermal reactions of diatomic [Cu−C]$^+$ with methane. In contrast, only a stepwise mechanism was found for the related [Au−C]$^+$/CH$_4$ couple. The root cause of this switch from a concerted to a stepwise mechanism can be attributed to the rather different BDEs of [M−C]$^+$ (M = Cu and Au). In addition, arguments are provided showing that the copper ion in the ethylene forming reaction of [Cu−C]$^+$ with methane can be replaced by a positive point charge; thus, the term "charge-induced catalysis" is suggested.

■ ASSOCIATED CONTENT

⑤ Supporting Information

The Supporting Information is available free of charge on the ACS Publications website at DOI: 10.1021/jacs.6b12514.

> Experimental and computational details, additional potential energy surfaces, energetic information, schematic molecular orbital diagrams, NBO-calculated charge and spin density mentioned in the main text, orbital components of ^{1}[Cu−C]$^+$ and ^{1}[Au−C]$^+$, plot of the influence of a point charge, plot of deformation energies vs the corresponding barriers, and Cartesian coordinates for key calculated species(PDF)

■ AUTHOR INFORMATION

Corresponding Authors

*E-mail: Jilai@jlu.edu.cn.
*E-mail: Sason@yfaat.ch.huji.ac.il.
*E-mail: Helmut.Schwarz@tu-berlin.de.

ORCID ⓘ

Jilai Li: 0000-0002-3363-9164
Sason Shaik: 0000-0001-7643-9421
Helmut Schwarz: 0000-0002-3369-7997

Notes

The authors declare no competing financial interest.

REFERENCES

(1) Olivos-Suarez, A. I.; Szécsényi, À.; Hensen, E. J. M.; Ruiz-Martinez, J.; Pidko, E. A.; Gascon, J. *ACS Catal.* **2016**, *6*, 2965−2981.

(2) Olah, G. A.; Goeppert, A.; Prakash, G. K. S. *Beyond Oil and Gas: The Methanol Economy*; Wiley-VCH: Weinheim, Germany, 2006.

(3) Roithová, J.; Schröder, D. *Chem. Rev.* **2010**, *110*, 1170−1211.

(4) Copéret, C. *Chem. Rev.* **2010**, *110*, 656−680.

(5) Balcells, D.; Clot, E.; Eisenstein, O. *Chem. Rev.* **2010**, *110*, 749−823.

(6) Schröder, D.; Schwarz, H. *Proc. Natl. Acad. Sci. U. S. A.* **2008**, *105*, 18114−18119.

(7) Mas-Balleste, R.; Que, L., Jr. *Science* **2006**, *312*, 1885−1886.

(8) Labinger, J. A.; Bercaw, J. E. *Nature* **2002**, *417*, 507−514.

(9) Crabtree, R. H. *Chem. Rev.* **1995**, *95*, 2599−2599.

(10) Lunsford, J. H. *Angew. Chem., Int. Ed. Engl.* **1995**, *34*, 970−980.

(11) Dietl, N.; Schlangen, M.; Schwarz, H. *Angew. Chem., Int. Ed.* **2012**, *51*, 5544−5555.

(12) Crabtree, R. H. *Nat. Chem.* **2009**, *1*, 348−349.

(13) Li, J.; Zhou, S.; Zhang, J.; Schlangen, M.; Usharani, D.; Shaik, S.; Schwarz, H. *J. Am. Chem. Soc.* **2016**, *138*, 11368−11377.

(14) Li, J.; Zhou, S.; Zhang, J.; Schlangen, M.; Weiske, T.; Usharani, D.; Shaik, S.; Schwarz, H. *J. Am. Chem. Soc.* **2016**, *138*, 7973−7981.

(15) Li, J.; Zhou, S.; Schlangen, M.; Weiske, T.; Schwarz, H. *Angew. Chem., Int. Ed.* **2016**, *55*, 13072−13075.

(16) Shevlin, P. B. Atomic Carbon. In *Reactive Intermediate Chemistry*; Moss, R. A., Platz, M. S., Jones, M., Jr., Eds.; John Wiley & Sons, Inc, 2005; pp 463−500.

(17) Leonori, F.; Skouteris, D.; Petrucci, R.; Casavecchia, P.; Rosi, M.; Balucani, N. *J. Chem. Phys.* **2013**, *138*, 024311.

(18) Jeong, G. H.; Klabunde, K. J.; Pan, O. G.; Paul, G. C.; Shevlin, P. B. *J. Am. Chem. Soc.* **1989**, *111*, 8784−8790.

(19) Kim, G.-S.; Nguyen, T. L.; Mebel, A. M.; Lin, S. H.; Nguyen, M. T. *J. Phys. Chem. A* **2003**, *107*, 1788−1796.

(20) Schröder, D.; Schwarz, H. *Angew. Chem., Int. Ed. Engl.* **1995**, *34*, 1973−1995.

(21) Schwarz, H. *Isr. J. Chem.* **2014**, *54*, 1413−1431.

(22) Taylor, H. S. *J. Phys. Chem.* **1926**, *30*, 145−171.

(23) Taylor, H. S. *Proc. R. Soc. London, Ser. A* **1925**, *108*, 105−111.

(24) Niu, D.; Willoughby, P. H.; Woods, B. P.; Baire, B.; Hoye, T. R. *Nature* **2013**, *501*, 531−534.

(25) Aragonès, A. C.; Haworth, N. L.; Darwish, N.; Ciampi, S.; Bloomfield, N. J.; Wallace, G. G.; Diez-Perez, I.; Coote, M. L. *Nature* **2016**, *531*, 88−91.

(26) Meir, R.; Chen, H.; Lai, W.; Shaik, S. *ChemPhysChem* **2010**, *11*, 301−310.

(27) Lai, W.; Chen, H.; Cho, K.-B.; Shaik, S. *J. Phys. Chem. Lett.* **2010**, *1*, 2082−2087.

(28) Hirao, H.; Chen, H.; Carvajal, M. A.; Wang, Y.; Shaik, S. *J. Am. Chem. Soc.* **2008**, *130*, 3319−3327.

(29) Shaik, S.; de Visser, S. P.; Kumar, D. *J. Am. Chem. Soc.* **2004**, *126*, 11746−11749.

(30) Kummerlöwe, G.; Beyer, M. K. *Int. J. Mass Spectrom.* **2005**, *244*, 84−90.

(31) Su, T.; Bowers, M. T. *J. Chem. Phys.* **1973**, *58*, 3027−3037.

(32) Bowers, M. T.; Laudenslager, J. B. *J. Chem. Phys.* **1972**, *56*, 4711−4712.

(33) Schröder, D.; Shaik, S. S.; Schwarz, H. *Acc. Chem. Res.* **2000**, *33*, 139−145.

(34) Harvey, J. N.; Aschi, M.; Schwarz, H.; Koch, W. *Theor. Chem. Acc.* **1998**, *99*, 95−99.

(35) Schwarz, H. *Angew. Chem., Int. Ed.* **2003**, *42*, 4442−4454.

(36) Pyykko, P.; Desclaux, J. P. *Acc. Chem. Res.* **1979**, *12*, 276−281.

(37) Wang, L.-S. *Phys. Chem. Chem. Phys.* **2010**, *12*, 8694−8705.

(38) Pauling, L. *J. Am. Chem. Soc.* **1932**, *54*, 3570−3582.

(39) Barysz, M.; Pyykkö, P. *Chem. Phys. Lett.* **1998**, *285*, 398−403.

(40) Ye, S.; Geng, C.-Y.; Shaik, S.; Neese, F. *Phys. Chem. Chem. Phys.* **2013**, *15*, 8017−8030.

(41) Neese, F. *J. Am. Chem. Soc.* **2006**, *128*, 10213−10222.

(42) Shaik, S.; Shurki, A. *Angew. Chem., Int. Ed.* **1999**, *38*, 586−625.

(43) Harzmann, G. D.; Frisenda, R.; van der Zant, H. S. J.; Mayor, M. *Angew. Chem., Int. Ed.* **2015**, *54*, 13425−13430.

(44) Hiberty, P. C.; Megret, C.; Song, L.; Wu, W.; Shaik, S. *J. Am. Chem. Soc.* **2006**, *128*, 2836−2843.

(45) Shaik, S.; Mandal, D.; Ramanan, R. *Nat. Chem.* **2016**, *8*, 1091−1098.

(46) Klinska, M.; Smith, L. M.; Gryn'ova, G.; Banwell, M. G.; Coote, M. L. *Chem. Sci.* **2015**, *6*, 5623−5627.